Atmos. Chem. Phys., 12, 11647–11663, 2012
www.atmos-chem-phys.net/12/11647/2012/
doi:10.5194/acp-12-11647-2012

Atmospheric Chemistry and Physics

A multi-model assessment of the impact of sea spray geoengineering on cloud droplet number

K. J. Pringle[1], K. S. Carslaw[1], T. Fan[1], G.W. Mann[1], A. Hill[2], P. Stier[3], K. Zhang[4,5], and H. Tost[6]

[1]Institute for Climate and Atmospheric Science, University of Leeds, UK
[2]UK Met Office, Exeter, UK
[3]Atmospheric, Oceanic and Planetary Physics, University of Oxford, UK
[4]Max Planck Institute for Meteorology, Hamburg, Germany
[5]Pacific Northwest National Laboratory, Richland, Washington, USA
[6]Johannes-Gutenberg-University Mainz, Germany

Correspondence to: K. J. Pringle (kirsty@env.leeds.ac.uk)

Received: 24 February 2012 – Published in Atmos. Chem. Phys. Discuss.: 9 March 2012
Revised: 24 November 2012 – Accepted: 26 November 2012 – Published: 6 December 2012

Abstract. Artificially increasing the albedo of marine boundary layer clouds by the mechanical emission of sea spray aerosol has been proposed as a geoengineering technique to slow the warming caused by anthropogenic greenhouse gases. A previous global model study (Korhonen et al., 2010) found that only modest increases ($< 20\,\%$) and sometimes even decreases in cloud drop number (CDN) concentrations would result from emission scenarios calculated using a windspeed dependent geoengineering flux parameterisation. Here we extend that work to examine the conditions under which decreases in CDN can occur, and use three independent global models to quantify maximum achievable CDN changes. We find that decreases in CDN can occur when at least three of the following conditions are met: the injected particle number is $< 100\,\mathrm{cm}^{-3}$, the injected diameter is > 250–$300\,\mathrm{nm}$, the background aerosol loading is large ($\geq 150\,\mathrm{cm}^{-3}$) and the in-cloud updraught velocity is low ($< 0.2\,\mathrm{m\,s}^{-1}$). With lower background loadings and/or increased updraught velocity, significant increases in CDN can be achieved. None of the global models predict a decrease in CDN as a result of geoengineering, although there is considerable diversity in the calculated efficiency of geoengineering, which arises from the diversity in the simulated marine aerosol distributions. All three models show a small dependence of geoengineering efficiency on the injected particle size and the geometric standard deviation of the injected mode. However, the achievability of significant cloud drop enhancements is strongly dependent on the cloud updraught speed. With an updraught speed of $0.1\,\mathrm{m\,s}^{-1}$ a global mean CDN of $375\,\mathrm{cm}^{-3}$ (previously estimated to cancel the forcing caused by CO_2 doubling) is achievable in only about $50\,\%$ of grid boxes which have $> 50\,\%$ cloud cover, irrespective of the amount of aerosol injected. But at stronger updraft speeds ($0.2\,\mathrm{m\,s}^{-1}$), higher values of CDN are achievable due to the elevated in-cloud supersaturations. Achieving a value of $375\,\mathrm{cm}^{-3}$ in regions dominated by stratocumulus clouds with relatively weak updrafts cannot be attained regardless of the number of injected particles, thereby limiting the efficacy of sea spray geoengineering.

1 Introduction

Several geoengineering options have been proposed to slow the rate of warming due to the anthropogenic increases in greenhouse gases, including the modification of stratospheric aerosol (Crutzen, 2006) and artificially increasing the surface albedo (Akbari et al., 2009). Latham and Smith (1990) proposed that climate warming could be slowed by increasing the albedo of marine stratocumulus clouds through the injection of sea spray aerosol. The idea is to build unmanned vessels which could be used to pump large number concentrations of sea spray aerosol into the marine boundary layer (Salter et al., 2008). These particles would then increase the number concentration of cloud droplets in marine

stratus clouds, and thus, if a constant cloud liquid water path is assumed, increase the planetary albedo.

Most global modelling studies on sea spray geoengineering so far have examined the climate response to a prescribed enhanced cloud droplet number (CDN) concentration (Latham et al., 2008; Jones et al., 2009; Rasch et al., 2009, marine CDN concentrations set to 375 or 1000 cm^{-3} either globally, or in defined regions). These studies found that the prescribed enhanced CDN concentration was sufficient to offset a significant fraction of the warning due to anthropogenic greenhouse gases, but they did not address the feasibility of attaining the prescribed enhancement in CDN. Marine CDN concentrations range from approximately 200–300 cm^{-3} in polluted coastal regions to ≤ 40 cm^{-3} in remote region (e.g. Bennartz, 2007; Lu et al., 2007). Thus attaining a marine droplet concentration of 375 cm^{-3} is equivalent to a percentage increase in CDN from 87 % to over 800 %.

Using a sectional global aerosol microphysics model (GLOMAP-Bin, Spracklen et al., 2005), Korhonen et al. (2010) calculated the percentage change in CDN achieved from the injection of sea spray particles (with the injection rate calculated online as a function of wind speed) in four marine regions with extensive cloud cover. The Korhonen et al. (2010) study was the first to consider geoengineering from an online windspeed dependent emission rate through to the change in CDN and they found that the calculated emission rates resulted in a regional average change in CDN of ≤ 20 %, and in some areas it even resulted in a decrease in CDN (because the increased competition for water vapour between the activated aerosol suppressed the in-cloud maximum supersaturation). This decrease in CDN is in line with the finding of Ghan et al. (1998) who found that the additon of sea spray aerosol can decrease CDN when the updraft is low and there is a large background concentration of sulfate particles.

This change in CDN found in Korhonen et al. (2010) is clearly much less than the enhancement in CDN assumed in previous studies. Using the ECHAM5.5-HAM2 model, Partanen et al. (2012) used the same injection flux parameterisation as Korhonen et al. (2010) but found much larger increases in CDN, it is not clear why larger increases in CDN were found as the model used, the activation parameterisation and the assumed updraught velocity all changed between the two studies.

While the Korhonen et al. (2010) and Partanen et al. (2012) studies are useful assessments of the efficiency of sea spray geoengineering they are based on a particular scenario, for example a fixed injection size and updraught are assumed and although a range of injection numbers is considered the dependence of the increase in CDN on the number of particles injected is not explicitly examined. This makes it difficult to understand the reasons for a particular CDN response. A smaller than previously expected increase in CDN could occur for either of two reasons:

1. Insufficient enhancement of the aerosol concentration: if the online calculation of the aerosol injection, processing and loss resulted in only a relatively small increase in aerosol number then it follows that only a small change in the CDN concentration would be produced.

2. Insufficient activation of the additional aerosol: if the activation potential of the cloud is not sufficient to activate the additional aerosol then a large increase in CDN would not be produced, even if the enhancement of the aerosol number concentration is very large.

Understanding the limiting processes in sea spray geoengineering is important as insufficient enhancement of the aerosol number concentration could potentially be solved by technological advances. However, if it is the case that the additional aerosol particles are not activating, then there is an upper limit to the maximum enhancement of CDN possible, and that limit is lower than has previously been assumed. In this study we explore which of these processes dominates in order to understand the efficiency of sea spray engineering.

The ability of the injected aerosol to activate into cloud droplets depends on three factors: (i) the properties of the injected aerosol, (ii) the concentration of marine aerosol able to serve as cloud condensation nuclei and (iii) meteorological factors, especially the updraught velocity. Using a cloud parcel model, Bower et al. (2006) examined the activation efficiency of advertently introduced aerosol particles assuming a range of different marine aerosol concentrations, updraught velocities, injection diameters and injection number concentrations. They found the marine aerosol number concentration to be of most importance, with low aerosol number concentrations producing large enhancements in CDN. The calculated enhancement in CDN was found to be quite insensitive to the size of the emitted particles, suggesting that it may not be essential to select a particular emission size. This is in contrast to the work of Hobbs et al. (2000) who used in situ measurements to analyse the cloud response to ship emissions and found that the response of the cloud was affected by the size of the particles on emission. Bower et al. (2006) also found that increasing the assumed in-cloud updraught velocity from 0.2 to 1.0 m s^{-1} resulted in only a small change in ΔCDN as the CDN in both the geoengineered and non-geoengineered case increased.

Alterskjær et al. (2011) used CDN concentrations measured from MODIS to identify low CDN regions to target effective geoengineering regions and found that the area between 30° S and 30° N was particularly susceptible to cloud seeding. They also found that although increases in CDN occurred (with an injection of 10^{-9} kg m^2 s^{-1} of sea salt with a modal radius of 0.13 μm) a uniform concentration of 375 cm^{-3} was not reached.

The cloud response to a change in aerosol loading is highly complex and depends on the meteorological conditions, for example Wang et al. (2011) used a cloud resolving model to

investigate the response of the cloud to sea-spray geoengineering and found geoengineering to be inefficient when the cloud is strongly precipitating or heavily polluted but efficient under clean and non/weakly precipitating conditions. Other studies have examined the response of clouds to the injection of aerosol from ship plumes, these question the extent to which an increase in aerosol will result in an increase in cloud albedo as in addition the cloud liquid water, cloud depth and cloud lifetime may also be affected. For example, Segrin et al. (2007) found that the cloud liquid water path decreased in 60 % of clouds in response to an increase in aerosol loading. Coakley and Walsh (2002) found that in ship tracks liquid water was typically reduced by 15–20 %. Christensen and Stephens (2011) found that the response to a ship plume was different in closed and open cells within the stratocumulus cloud deck, with open cell clouds increasing in height in response to the increased aerosol. The albedo response to geoengineering is also affected by cloud lifetime, which may increase as a result of the reduced droplet size which reduces the drizzle rate (e.g. Christensen et al., 2009). Global climate models struggle to capture these complex interactions as they are limited both in terms of resolution and in the model complexity feasible, but a global view is required to assess the impact of changing CDN on the Earth's climate, e.g. on the changes to the meridional heat transport (Parkes et al., 2012) or changes in precipitation Jones et al. (e.g. 2009).

As the efficiency of sea spray geoengineering is sensitive to the marine aerosol distribution it is likely that the simulated efficiency will depend on the model used. In a global aerosol model the simulated marine distribution is a function of the sea spray emissions flux, outflow of aerosol from continental regions, microphysical processing and wet and dry deposition. All of these processes are uncertain and treatment varies between models (Textor et al., 2006). The diversity in model estimates of the background marine aerosol distribution may therefore affect the calculated efficiency of the sea-spray geoengineering, but this uncertainty has not yet been examined.

The aim of this paper is to explore the change in CDN that arises from the injection of sea-spray aerosol under a range of different conditions. This information is important as it can be used to understand if and how greater increases in CDN can be achieved. Understanding the limiting factors also helps to quantify the maximum possible increase in CDN (for macrophysically identical clouds) which is useful for studies that calculate the potential radiative cooling arising from sea-spray geoengineering.

2 Methods

We show results from multiple simulations of a microphysically based aerosol activation parametrisation (Nenes and Seinfeld, 2003; Fountoukis and Nenes, 2005; Barahona et al., 2010), hereafter referred to as BN10. The scheme has been shown to compare well against both cloud parcel calculations and in-situ observations (Fountoukis and Nenes, 2005; Meskhidze et al., 2005) and has been used extensively in global model studies (e.g. Chen and Penner, 2005; Pringle et al., 2009; Merikanto et al., 2010). The BN10 parametrisation is based on the framework of an ascending cloud parcel; the parametrisation calculates the maximum supersaturation (which controls CDN) from the balance of water vapour availability from cooling and the depletion from the condensational growth of activated droplets. In this paper we apply the BN10 parametrisation both to a "typical" marine aerosol distribution (Sect. 3) and to output from three global aerosol models (Sect. 4): GLOMAP-MODE (Global Model of Aerosol Processes Mann et al., 2010), the ECHAM-MESSy Atmospheric Chemistry model (EMAC, Jöckel et al., 2006; Pringle et al., 2010; Pozzer et al., 2012) and ECHAM-HAM (Stier et al., 2005).

The three models considered are fundamentally similar in that they all treat the aerosol size distribution using 7 log-normal modes (following Vignati et al., 2004), but they differ in their treatment of aerosol emission and deposition, two key factors affecting the global aerosol burden (Textor et al., 2006) and also in the chemistry schemes used. The GLOMAP microphysics routines were developed independently of the other two models (Mann et al., 2010; Spracklen et al., 2005), however ECHAM-HAM and EMAC share the same core microphysics routines, with the aerosol scheme in EMAC (GMXe) being a development of the M7 microphysics module in ECHAM-HAM (the GMXe code was adapted from the M7 to include nitrate aerosol, Pringle et al., 2010). In these simulations the GLOMAP and EMAC models use a horizontal resolution of T42 and ECHAM-HAM a resolution of T63. Both ECHAM-HAM and GLOMAP use 31 vertical levels and EMAC uses 19 levels in the vertical.

The model simulations are provided by the AeroCom aerosol model inter-comparison project (http://aerocom.met.no/Welcome.html/) and are representative of the year 2006. Two versions of ECHAM-HAM were submitted to the AeroCom Phase II Inter-comparison, one representative of the setup used in Stier et al. (2005, HAM1) and another from Zhang et al. (2012, HAM2). In this study we use the HAM1 results as the treatment of the aerosol composition in this model version is more comparable to GLOMAP-MODE and EMAC and the model is widely used.

In all simulations, the calculation of global fields of CDN is done offline (i.e. as a postprocessing step rather than during the model simulation) and the BN10 activation calculation is used to calculate CDN assuming a range of prescribed updraught velocities in every model gridbox. This approach means that the updraughts used in the CDN parameterisation are not the same as those used within the aerosol activation and wet removal parameterisations within the models. We take this approach as the models all have different aerosol activation and wet removal parameterisations thus the

Table 1. The accumulation mode background aerosol loading taken from Heintzenberg and Larssen (2004, HL04) and cloud droplet number concentration simulated using a range up updraught velocities. Subsequent rows; loadings used in the 0-D sensitivity tests. The second column shows the assumed number concentration of aerosol in the accumulation mode and the last four columns show the predicted CDN concentration in the absence of geoengineering (assuming a prescribed updraught, w).

Expt	Accumulation (cm^{-3})	CDN $w = 0.05$	CDN $w = 0.1$	CDN $w = 0.2$	CDN $w = 0.4$
HL04	98	60.4	83.9	101.4	121.9
HL04-025	25	25.5	32.7	48.6	77.2
HL04-050	50	39.8	50.7	63.3	89.6
HL04-067	67	47.5	62.5	75.3	99.4
HL04-150	150	78.0	110.6	140.17	160.9
HL04-200	200	101.3	133.6	175.68	202.7
HL04-400	400	116.4	210.7	298.62	364.3

assumed updraught velocity varies between models. It should also be noted that by using monthly mean aerosol fields we cannot capture the day to day variability of the aerosol distribution which could lead to biases in the predicted annual mean change in CDN, this is a limitiation of the offline approach used.

We do not restrict calculation of CDN to gridboxes that contain clouds; to achieve a global distribution a theoretical CDN is calculated in every model gridbox. The BN10 scheme is an activation parametrisation and does not allow for the calculation of in-cloud collision/coalescence and thus will tend to overestimate CDN concentrations compared to in situ observations (methodology is similar to that of Pringle et al., 2009; Merikanto et al., 2010; Korhonen et al., 2010; Karydis et al., 2011). This offline approach does not treat the entrainment of air at cloud top. By using an activation parameterisation we cannot capture any changes to the macrophysical properties of the cloud that occur as a result of the injected aerosol, thus we cannot calculate the resulting change in cloud albedo or forcing as a result of the geoengineering.

3 Exploring parameter space in a 0-D model

To understand the response of CDN to a range of injection scenarios, updraught velocities and background marine aerosol number concentrations the BN10 parametrisation was first run as a stand alone box model, or 0-D, version. The conditions are summarised in Tables 1 and 2 and described below. The aim of this work is to build on previous work by, e.g. Bower et al. (2006) and Ghan et al. (1998) by extending the region of parameter space examined in order to identify the optimum conditions for sea spray geoengineering in a simple scenario before global fields are considered.

Table 2. Regional mean increase in total aerosol number (cm^{-3}) at 1 km altitude arising from sea spray geoengineering as calculated using the simulation of Korhonen et al. (2010).

Area	Geo	St Dev	5*Geo	St Dev
North Pacific	69.80	13.51	363.10	60.78
South Pacific	66.33	5.10	362.70	30.78
South Atlantic	76.72	7.68	401.70	36.24
Indian Ocean	62.02	10.90	334.04	49.77
Average	68.72	9.30	365.38	44.39

3.1 Conditions examined

3.1.1 Injected aerosol properties

Using a wind speed dependent injection parametrisation based on literature estimates of the efficiency of the proposed vessels, Korhonen et al. (2010) simulated the injection of sea spray aerosol online in a global aerosol model in four marine regions. In the baseline simulation they calculated an annual mean increase in aerosol number across the four regions of $68.72 \pm 13.51\,cm^{-3}$ at 1 km altitude. They also considered a sensitivity scenario in which the emission flux was increased by a factor of 5, leading to an increase in aerosol number of $365.38 \pm 44.39\,cm^{-3}$ (H. Korhonen, personal communication, 2011, see Table 2), this implies that the enhancement in aerosol number scales almost linearly with the mass flux. Throughout this paper we use the simulated increase in aerosol number from Korhonen et al. (2010) as an estimate of $1\times$ and $5\times$ geoengineering scenarios. In the 0-D-section we consider scenarios in which the additional number increases stepwise from 0 to $500\,cm^{-3}$, the Korhonen et al. (2010) estimates are at the lower and middle region of this parameter space.

In all simulations shown in this work, the additional aerosol is assumed to simply add to the background aerosol distribution; we do not simulate the change in the pre-existing marine aerosol distribution due to the presence of additional aerosol. This is a simplification as the additional aerosol may interact with the pre-existing aerosol,e.g. through coagulation, but it is justified on the basis that Korhonen et al. (2010) found the impact of the additional aerosol on the pre-aerosol distribution to be small as coagulation rates are slow at these sizes.

3.1.2 Background aerosol concentration

To explore the sensitivity to the pre-exisiting marine aerosol loading we assume a baseline aerosol size distribution taken from the Heintzenberg and Larssen (2004, HL04) remote marine aerosol climatology (Table 1). In this climatology the modal geometric standard deviation is 1.4 for all modes, the mode diameters are 43, 149 and 487 nm and the number

Table 3. Summary of updraught velocities calculated in an LEM simulation for the ASTEX GCSS Sc-Cu transition case. The final column shows the percentage of updraughts that are greater than the reference updraught velocity (w)

Time	Location	Updraught (w)	$\% > w$
Night	Cloud Base	0.05	87.93
Night	Cloud Base	0.10	76.26
Night	Cloud Base	0.20	55.37
Night	Cloud Base	0.40	26.35
Night	Cloud Base	0.60	11.78
Night	Cloud Base	0.80	5.24
Night	Cloud Base	1.00	2.29
Day	Cloud Base	0.05	84.26
Day	Cloud Base	0.10	70.24
Day	Cloud Base	0.20	47.79
Day	Cloud Base	0.40	22.33
Day	Cloud Base	0.60	10.73
Day	Cloud Base	0.80	4.96
Day	Cloud Base	1.00	2.03

concentrations are 146, 98 and 4 cm^{-3}. A series of initial sensitivity studies was performed and we found that at the updraughts considered, the number concentration of aerosol in the accumulation mode was the most important feature of the background aerosol size distribution in affecting the sensitivity to the geoengineered aerosol. Simulations are therefore preformed assuming a range of accumulation mode number loadings (see Table 1). At larger updraughts, the CDN becomes increasingly sensitive to Aitken mode particles as well, but in marine stratocumulus updraughts the effect of the accumulation mode dominates. For simplicity we take an accumulation number concentration of 100 cm^{-3}, a slight increase (3 cm^{-3}) on the 97 cm^{-3} presented by HL04 (the concentrations of the other modes are from HL04).

3.1.3 In-cloud updraught velocity

Updraught velocity varies both between and within marine stratocumulus cloud decks (e.g. Hawkins et al., 2008; Bretherton et al., 2010; Rahn and Garreaud, 2010). Measurements show a distribution of updraughts that peaks at (or near) zero, but the variance and the skewness of the distribution varies. Vertical velocity is typically smaller at cloud base but increases with height until reaching a maximum around (or above) the centre of the cloud (Lu and Seinfeld, 2005, 2006; Hill et al., 2009). The velocity in the lower levels of the cloud is of most interest for this work as it is mainly these values that control the cloud droplet number concentration: activation starts close to cloud base and once a spectrum of cloud droplets has been formed additional condensation will tend to grow cloud droplets rather than activate additional aerosol.

Field observations of updraft velocity report either the standard deviation of the updraught (σ_w) or a single average or characteristic updraught value (w), in this document, unless otherwise stated we refer to updraught as a single characteristic values (although we calculate the global fields using a PDF of updraughts (σ_w)). Peng et al. (2005) suggest a conversion factor of 0.8 to convert the PDF to a single characteristic updraught ($w = 0.8\sigma_w$) and Morales and Nenes (2010) found that a conversion factor of 0.65 fits best for calculation of CDN.

Marine stratocumulus updraughts are generally quite low, for example Guo et al. (2008) present PDFs of vertical velocity in marine stratocumulus clouds measured during the Marine Stratus/Stratocumulus Experiment (MASE), they found that characteristic updraughts (w) were always $< 0.2\,\mathrm{m\,s}^{-1}$ at the middle and base of the cloud, but found slightly higher updraughts close to the cloud top. Guibert et al. (2003) reported an average updraught velocity of $0.16\,\mathrm{m\,s}^{-1}$ and flight mean maximum value of $0.33\,\mathrm{m\,s}^{-1}$ during the ACE-2 CLOUDYCOLUMN experiment in stratocumulus clouds in the eastern Atlantic Ocean. Lu et al. (2007) found an average updraught velocity of $0.18\,\mathrm{m\,s}^{-1}$ in marine stratocumulus clouds off the coast of California, USA. Larger in-cloud updraught velocities were found in the Southeastern Pacific during the VOCALS (VAMOS Ocean-Cloud-Atmosphere-Land Study) campaign, Bretherton et al. (2010) found sub-cloud values of $\sigma_w = 0.3$–$0.5\,\mathrm{m\,s}^{-2}$ (or $w = 0.24$–$0.40\,\mathrm{m\,s}^{-1}$) in-cloud values of $\sigma_w = 0.2$–$0.8\,\mathrm{m\,s}^{-2}$ (or $w = 0.16$–$0.64\,\mathrm{m\,s}^{-1}$).

Table 3 shows frequency statistics for the updraught (w) simulated in the UK Met Office Large-Eddy Simulation Model (LEM, 3-D) for the ASTEX GCSS Sc-Cu transition case (Bretherton et al., 1999) (A. Lock, personal communication, 2011). This model simulation represents a range of marine stratocumulus updraught velocities including (during the daytime) some transition from stratocumulus into cumulus clouds, which have higher updraught. In this case 27 % of updraughts were $< 0.1\,\mathrm{m\,s}^{-1}$, 49 % were $< 0.2\,\mathrm{m\,s}^{-1}$ and 75 % of updraughts were $< 0.4\,\mathrm{m\,s}^{-1}$. In this work we adopt $0.4\,\mathrm{m\,s}^{-1}$ an upper limit for consideration but note that larger updraughts do occur in marine stratocumulus clouds, especially when they start to transition into cumulus clouds.

3.2 Results of the 0-D simulations

Figure 1 shows the percentage change in CDN arising from the injection of a single sea spray aerosol mode with a geometric standard deviation of 1.1, climatological marine aerosol distribution from Heintzenberg and Larssen (2004) and an in-cloud updraught velocity (w) of $0.1\,\mathrm{m\,s}^{-1}$. We present the percentage change in CDN because in the Twomey (1977, 1991) framework, the change in cloud albedo is proportional to the percentage (not absolute) change in CDN, when cloud liquid water is constant. The shape of the distribution in Fig. 1 helps identify optimum

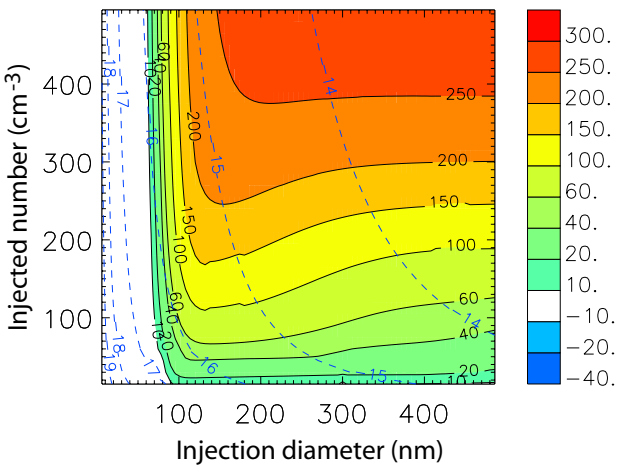

Fig. 1. The percentage change in CDN that occurs upon the injection of a sea spray mode with geometric standard deviation of 1.1 and with diameter shown on the x-axis and injected mode number shown on the y-axis. Calculations assume a background aerosol distribution taken from Heintzenberg and Larssen (2004, HL04) and an updraught velocity of 0.1 m s^{-1}. Blue dashed lines show the $\log_{10}$ of the mass of the injected aerosol, e.g. the −14 contour corresponds to a injected aerosol mass of 1×10^{-14} kg cm^{-3}.

conditions for geoengineering, for example if the number of injected particles is fixed, e.g. at 250 cm^{-3} then injecting at 150 nm diameter produces the largest increase in CDN. If the injection size is increased away from this optimum diameter (i.e. the injection number is held constant but the mass injected increased) then geoengineering becomes less effective (smaller change in CDN) as the large particles are an effective sink for condensation and the maximum supersaturation is suppressed. Conversely, when the injection diameter is reduced from the optimum then a fraction of the narrow mode becomes too small to activate and the increase in CDN is reduced. In the scenario considered in Fig. 1 the advertently introduced aerosol results in an increase in CDN providing the injected particle diameter is > 90 nm (below this size the increase in CDN is ≤ 10 %) and the injection diameter at which the greatest enhancement in CDN occurs ranges from 100–200 nm depending on the number of advertently introduced particles.

Figure 1 shows that under this scenario of clean marine background aerosol loading large enhancements in CDN can be readily achieved, Fig. 2 extends this analysis to other background aerosol loadings and updraughts. Each panel is a repeat of the plot in Fig. 1, but calculated assuming different in-cloud updraught velocities (w) and increased background aerosol number concentration. Independent of the in-cloud updraught velocity, the increase in CDN becomes smaller when more accumulation mode particles exist in the background distribution (e.g. when the sea spray flux is large, or when close to pollution sources). If the background aerosol loading is reduced to loadings lower than that presented by Heintzenberg and Larssen (2004) then the increase in CDN becomes larger and very little dependence on injection size is apparent (not shown). This dependence on background aerosol loading can be understood by considering the degree of competition for water vapour; when the background aerosol loading is large there is increased competition for water vapour and thus a reduced fraction of the advertently introduced aerosol can activate to form cloud droplets, resulting in a reduced efficiency of the geoengineering. The dependence of the percentage change in CDN on the injected diameter is more complex; injecting at a diameter of 150 to 300 nm results in the largest increases in CDN, but the exact value within this range depends on the both the pre-existing aerosol loading and the updraught. The value of 260 nm used in previous studies was well chosen as an efficient size, but greater enhancements in CDN can sometimes be achieved by injecting at a diameter of 150–200 nm (discussion continued in Sect. 4.1).

We repeated these experiments assuming a geometric standard deviation of 1.3 and 1.6 (not shown). With the wider modes the pattern of the change in CDN is similar but the wider mode reduces the CDN achieved (fewer particles activate) unless the injection diameter is very small, in which case the wide mode increases the fraction of the mode where particles are large enough to activate.

Figure 2 also shows the importance of the in-cloud updraught velocity for effective geoengineering. When updraught is 0.4 m s^{-1} the advertently introduced aerosol increases CDN even when the background aerosol loading is large. But when updraught is low ($w \leq 0.2$ m s^{-1}), the competition between the activation of the background and advertently introduced aerosol becomes important and the percentage increase in CDN achieved remains small. It is important to note that separately low updraught or high background loading may not prohibit the activation of the additional aerosol (although they do reduce the efficiency), but these factors combined result in only a small change in CDN. From Fig. 2, we find that a decrease in CDN occurs when at least three of the following conditions are met:

1. The injected particle number is low (≤ 150 cm^{-3}).
2. Injected particle diameter is large ($\geq$ 250–300 nm).
3. The background accumulation mode number loading is large (≥ 150 cm^{-3}).
4. The in-cloud updraught velocity is low ($w \leq 0.2$ m s^{-1}).

Korhonen et al. (2010) found that injecting approximately 70 cm^{-3} particles of 260 nm in diameter could result in a net decrease in CDN over large spatial scales, the above analysis confirms that reductions in CDN can occur in this region of the parameter space. For the conditions examined, decreases in CDN can generally be avoided by injecting more particles and injecting at a smaller diameter.

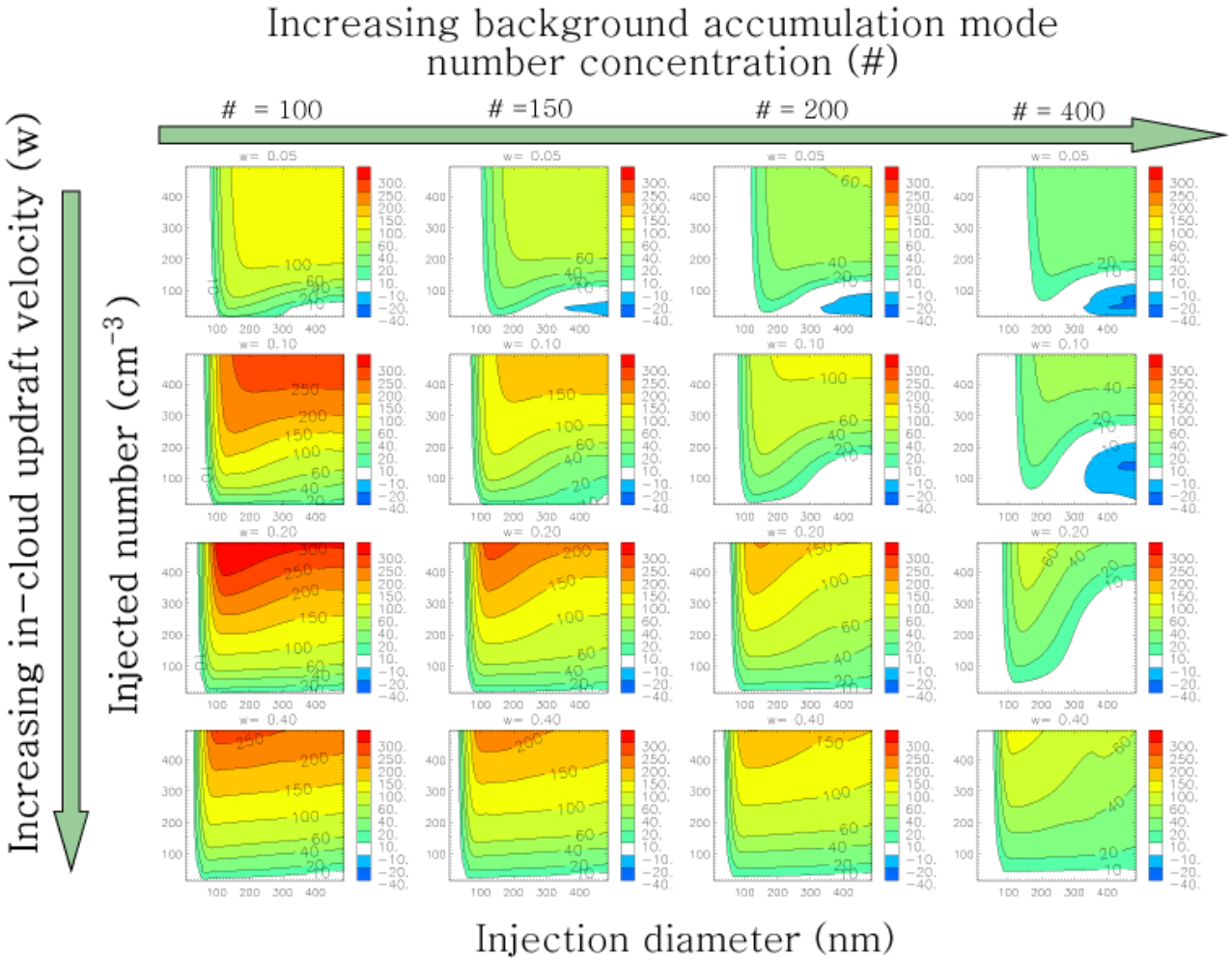

Fig. 2. The percentage change in CDN that occurs upon the injection of a sea spray mode with geometric standard deviation of 1.1 and with diameter shown on the x-axis and injected mode number shown on the y-axis of each panel. Rows show plots with constant updraught velocity but increasing accumulation mode number concentration (left to right; 100, 150, 200 and 400 cm^{-3}). Updraught velocity increases down a column (top row $w = 0.05$; second top row $w = 0.01$; second bottom row $w = 0.2$; bottom row $w = 0.4\,\mathrm{m\,s^{-1}}$).

4 Efficiency of sea spray geoengineering: results from multiple models

In this section we take output from three global aerosol models: GLOMAP-MODE (Mann et al., 2010), EMAC (Pringle et al., 2010) and ECHAM-HAM (Stier et al., 2005) and calculate global fields of CDN predicted from each model with and without sea spray geoengineering. The model simulations are from the AeroCom model inter-comparison project (http://aerocom.met.no/Welcome.html) which provides monthly mean output representative of the year 2006. The calculation of aerosol activation was done offline, allowing different assumptions about the size and number of aerosol added. Geoengineered aerosol is added uniformly across a gridbox and is assumed not to affect the background aerosol distribution. Fields of CDN are calculated at an average altitude of 940 hPa, representative of cloud base. A schematic of the methodology is shown in Fig. 3. In these simulation a Gaussian PDF of updraughts is assumed to occur in every model gridbox ($\sigma_w = 0.25$, mean $= 0.0$): CDN is calculated for multiple (10) updraughts within this PDF then a mean CDN is calculated from a probability weighted mean of these values, this is a similar approach to Korhonen et al. (2010). Also following Korhonen et al. (2010), aerosol is injected with a diameter of 260 nm. The three aerosol models are similar in that they treat the aerosol size distribution as the supposition of lognormal modes and they treat sulfate, mineral dust, black carbon, organic carbon and sea spray (and nitrate treated by EMAC only), but they differ in the treatment of sea spray emission and aerosol wet and dry deposition. All models used the same criteria to distinguish between the four size categories: nucleation (< 5 nm), Aitken (5–50 nm),

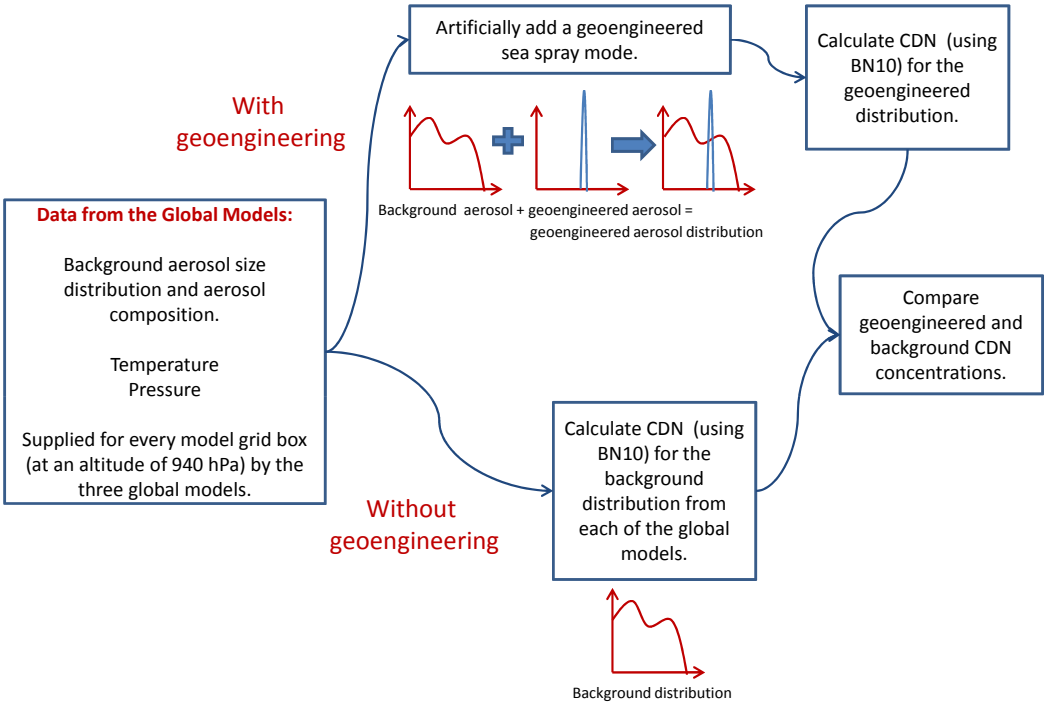

Fig. 3. Schematic summarising the methodology by which background and geoengineered CDN concentrations are calculated from the output of the 3 global aerosol models. BN10 is the parametrisation of Nenes and Seinfeld (2003); Barahona et al. (2010).

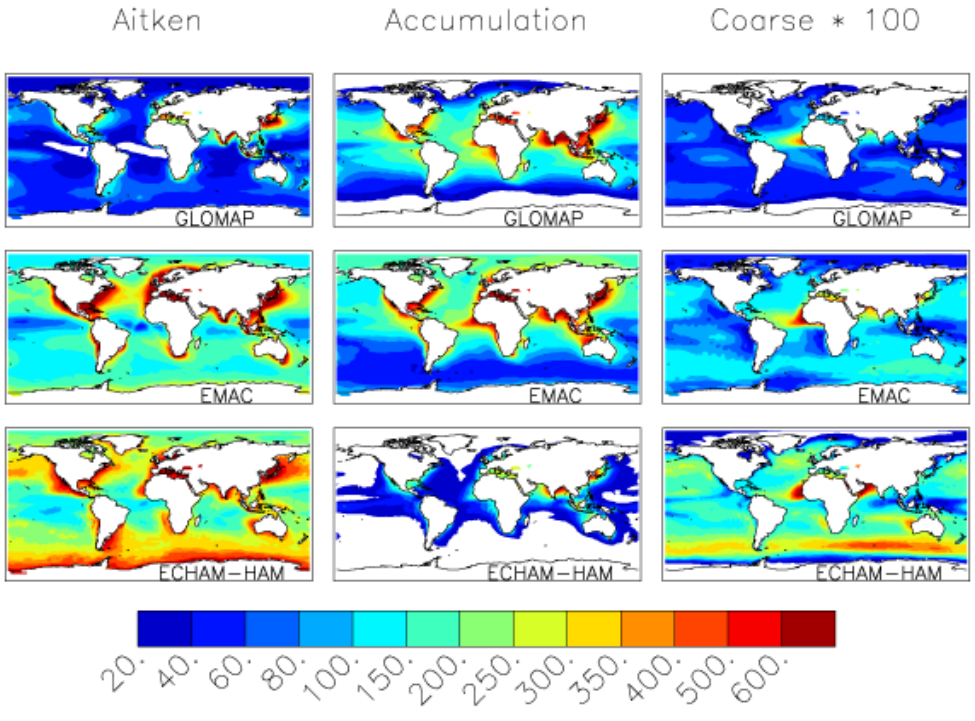

Fig. 4. Annual mean simulated marine hydrophilic aerosol number concentration (cm^{-3}) in the Aitken (5–50 nm), accumulation (50–500 nm) and coarse (> 500 nm) hydrophilic modes in (i) top row: GLOMAP; (ii) middle row: EMAC and (iii) bottom row: ECHAM-HAM. Data for all models is for an average altitude of 940 hPa.

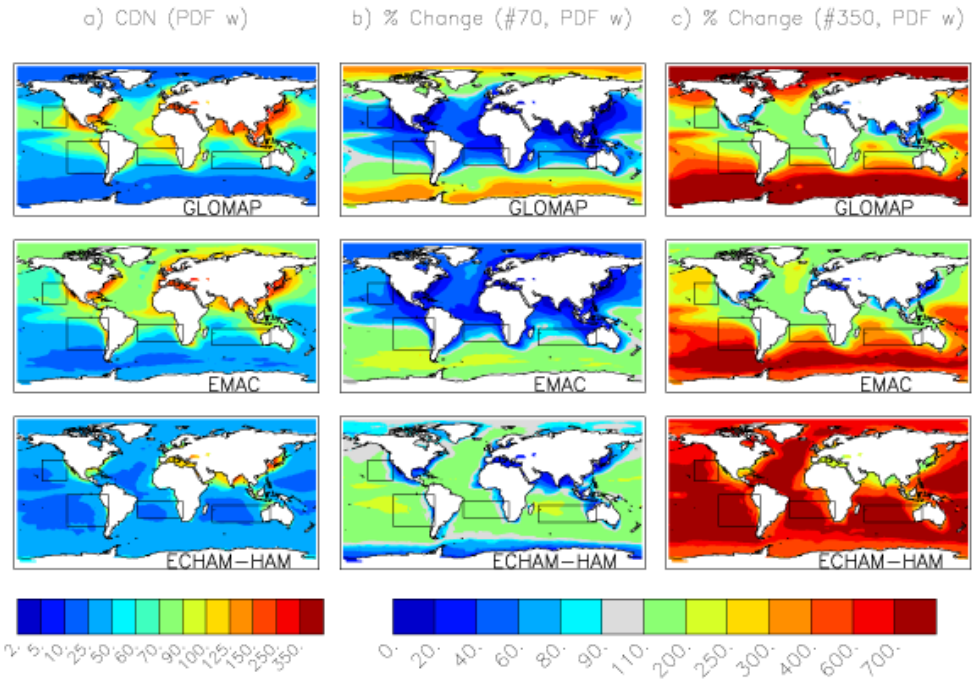

Fig. 5. (a) annual mean simulated marine cloud droplet number concentration (cm^{-3}) in the absence of geoengineering, **(b)** percentage change in CDN arising from sea spray geoengineering assuming the injection of 70 particles cm^{-3} and **(c)** percentage change in CDN arising from sea spray geoengineering assuming the injection of 350 particles cm^{-3} in the three models (top row: GLOMAP; middle row: EMAC and bottom row: ECHAM-HAM). CDN calculations assume a Gaussian PDF of updraught velocities with a standard deviation = 0.25, mean = 0.0.

accumulation (50–500 nm) and coarse (> 500 nm) dry radius (see Table 4 for a summary of the models). In the figures shown in this paper, we calculate the total number of aerosol in a size category for each model by integrating the number concentration of hydrophilic aerosol between the mode boundaries (e.g. for Aitken we count the total number of aerosol particles with dry radius ($5 < R_p < 50$ nm).

Figure 4 shows the annual mean simulated marine aerosol number concentration in the Aitken, accumulation and coarse hydrophilic modes in the three models. There is considerable diversity in the simulated number concentrations. ECHAM-HAM and EMAC both predict Aitken mode number concentrations of $> 200\,cm^{-3}$ over most marine regions but GLOMAP predicts lower values (40–200 cm^{-3}). The difference in Aitken mode number is especially pronounced in remote regions and in the Southern Ocean where ECHAM-HAM (and to a lesser extent EMAC) show high Aitken mode number concentrations near the Antarctic coast. Conversely, GLOMAP and EMAC have larger accumulation mode number concentrations than ECHAM-HAM with concentrations of $> 100\,cm^{-3}$ over most of the Northern Hemisphere compared to the ECHAM-HAM value of $< 60\,cm^{-3}$. ECHAM-HAM has a higher concentration of coarse mode particles than the other models. It should be noted that the difference in Aitken and accumulation mode number concentrations between the three models is less in the surface layer where more comprehensive measurements allow better model evaluation than at the low cloud base altitude considered here.

The simulated fields of CDN calculated offline from the model output are shown in Fig. 5, left column. In this figure we assume a PDF of updraughts (σ_w) with a standard deviation of 0.25 and a mean of 0. As we do not treat collision/coalescence this field actually represents the number of aerosol that would activate in the model if that updraught occurred rather than the absolute number of droplets that would be observed by measurements, but as the number of activated aerosol drives the in-cloud droplet concentration it is a useful metric for considering the response of the cloud to a perturbation. In this text we use the term CDN for the number of aerosol activated.

The GLOMAP and EMAC models predict similar global mean marine CDN concentrations (Table 5), but ECHAM-HAM predicts consistently lower values as a consequence of the lower accumulation mode concentrations in ECHAM-HAM. The distribution of CDN also varies significantly between the three models. GLOMAP simulates the strongest contrast in CDN between the polluted continental outflow regions ($CDN > 80\,cm^{-3}$), which extend a significant distance over the ocean, and very low CDN concentrations (10–25 cm^{-3}) in the Arctic and the remote Southern Ocean.

Table 4. Summary of the 4 aerosol models used.

Model	Host model	Sea Spray Emissions	Sea Spray Parametrisation	Reference
GLOMAP MODE	CTM	Online	Gong (2003)	Mann et al. (2010)
ECHAM-HAM	GCM (nudged)	Online	Monahan et al. (1986)	Stier et al. (2005)
EMAC	GCM (nudged)	Offline	Dentener (2006)	Pringle et al. (2010)

Table 5. Summary of the simulated annual mean background CDN concentration (without geoengineering) globally and in the four target geoengineering regions. CDN concentrations are calculated using the updraught velocity shown in the first column.

Updraught ($m\,s^{-1}$)	GLOMAP	EMAC	ECHAM-HAM
Global Mean			
0.05	50.91	54.90	24.03
0.10	71.90	74.43	33.98
0.20	92.20	93.56	49.32
0.40	110.81	110.30	72.39
N. Pacific			
0.05	86.62	74.27	29.06
0.10	112.04	92.70	35.21
0.20	139.36	107.11	48.29
0.40	160.34	115.04	70.47
S. Pacific			
0.05	83.67	54.69	28.06
0.10	119.88	71.33	35.21
0.20	148.25	85.36	48.29
0.40	168.27	97.12	70.47
S. Atlantic			
0.05	94.95	72.99	27.91
0.10	141.34	97.71	34.56
0.20	174.63	120.44	48.32
0.40	201.29	135.41	72.76
Indonesian Ocean			
0.05	81.49	56.64	21.37
0.10	106.91	68.43	28.97
0.20	127.63	76.07	43.96
0.40	140.36	81.24	68.86

EMAC predicts a much more homogeneous distribution, with CDN concentrations of 60–100 cm^{-3} over much of the Northern Hemisphere, including much of the Arctic. ECHAM-HAM shows a much lower CDN concentration in continental outflow regions than the other models, but simulates a slightly larger Southern Ocean CDN concentration than the other models (30–50 cm^{-3}).

During the VOCALS Regional Experiment in the Southeast Pacific Bretherton et al. (2010) measured CDN concentrations of $> 200\,cm^{-3}$ close to the western coast of South America (probably due to the high sulfur emissions from Copper smelting in this area), with concentrations dropping to $< 100\,cm^{-3}$ west of 80° W. Compared to this, ECHAM-HAM underestimates the CDN concentration close to coast with no values $> 100\,cm^{-3}$ but it captures the low CDN concentrations further from the coast. Conversely GLOMAP (and to a lesser extent EMAC) captures the region of high CDN but overestimates the region of high CDN; the high values extend further from the coast than in the observations. Bennartz (2007) presented CDN fields from MODIS and found a South Pacific mean CDN concentration of $40\,cm^{-3}$ which is broadly in line with ECHAM-HAM, but a lower value than the other two models. ECHAM-HAM underestimates CDN in the North Atlantic compared to Bennartz (2007, $89\,cm^{-3}$) as they never simulate concentrations $> 50\,cm^{-3}$ but EMAC and GLOMAP perform better in this region (CDN = 70–90 cm^{-3}). EMAC and GLOMAP both overestimate North Pacific concentrations ($64\,cm^{-3}$) but ECHAM-HAM tends to underestimate CDN concentrations in this region. In summary all models perform reasonably compared to large-scale observations but GLOMAP and EMAC tend to overestimate polluted marine concentrations and ECHAM-HAM tends to underestimate in these regions.

The central and right hand columns of Fig. 5 show the percentage increase in CDN caused by the addition of 70 (middle column) and 350 (right column) particles cm^{-3} to every marine gridbox in each of the three models. With the addition of 70 particles cm^{-3} (1 × geoscenario) ECHAM-HAM predicts that nearly all regions experience an increase in CDN of 110–200 %, but EMAC and GLOMAP suggest that changes of 110–200 % are only attainable over Southern Ocean (and the Arctic in GLOMAP only). In all models the pattern of the percentage change broadly reflects the inverse of the unperturbed CDN fields, with low initial CDN concentrations producing large percentage changes. This is partly due to the fact that low initial CDN concentrations mean that there is less competition for aerosol water and therefore more activation of the additional aerosol, and partly because the same absolute change will result in a larger percentage change if the initial value is smaller.

With the addition of 350 particles cm^{-3} (5 × geoscenario) the models all predict that considerable increases in CDN are possible over large regions. GLOMAP and EMAC both predict increases in CDN of 300–400 % in much of the Southern Ocean, and > 110 % in much of the Tropics and Northern Hemisphere. ECHAM-HAM predicts a more uniform distribution with changes of at least > 400 % in all regions with changes of > 700 % in most remote regions. In all models, regions of high aerosol loading resulting from continental outflow can decrease the efficiency of the geoengineering

Table 6. Summary of the regional background (NoGeo), geoengineered (Geo) and percentage change (%) in CDN arising from the injection of a range of sea spray number concentration (Inj number: 100, 200, 400 and 600 cm^{-3}, left column). A PDF of updraughts with $\sigma_w = 0.25$, mean = 0 is assumed.

	NoGeo N. Pac	Geo N. Pac	% N. Pac	NoGeo S. Pac	Geo S. Pac	% S. Pac	NoGeo S. Atl	Geo S. Atl	% S. Atl	NoGeo Ind. O.	Geo Ind. O	% Ind. O
GLOMAP												
100	69.50	108.34	55.89	73.86	107.79	45.94	86.62	120.73	39.38	63.45	102.36	61.32
200	69.50	143.63	106.67	73.86	138.55	87.58	86.62	149.21	72.25	63.45	137.44	116.60
400	69.50	222.06	219.52	73.86	208.35	182.08	86.62	219.41	153.30	63.45	213.74	236.86
600	69.50	301.73	334.15	73.86	266.53	260.86	86.62	277.52	220.38	63.45	280.40	341.91
EMAC												
100	53.33	96.29	80.55	42.74	80.38	88.06	59.88	97.32	62.52	38.08	80.91	112.50
200	53.33	136.85	156.59	42.74	117.36	174.59	59.88	131.75	120.02	38.08	121.94	220.26
400	53.33	220.69	313.80	42.74	195.24	356.81	59.88	208.76	248.62	38.08	205.56	439.88
600	53.33	302.20	466.64	42.74	265.02	520.06	59.88	277.68	363.72	38.08	277.58	629.02
ECHAM-HAM												
100	27.86	63.95	129.56	24.99	62.28	149.21	25.12	63.04	150.95	22.88	59.81	161.41
200	27.86	110.16	295.40	24.99	105.66	322.75	25.12	107.06	326.22	22.88	104.37	356.18
400	27.86	205.23	636.68	24.99	193.63	674.74	25.12	196.51	682.29	22.88	195.32	753.74
600	27.86	292.05	948.32	24.99	265.73	963.21	25.12	267.59	965.28	22.88	269.48	1077.88

to $< 110\,\%$, but in ECHAM-HAM this occurs only in the $1\times$ geoscenario and in quite a small region (the west of Africa and in coastal regions south of Asia and Indonesia). In GLOMAP and EMAC there are more regions which experience a small increase in CDN, with coastal regions near N. and S. America and East of China also experiencing an increase in CDN of $< 110\,\%$ even in the $5\times$ geoengineering scenario.

The simulated changes within four previously identified target geoengineering regions (marked as rectangles in Fig. 5) are summarised in Table 6 and can be compared to those predicted by Korhonen et al. (2010) with the GLOMAP-Bin model. Korhonen et al. (2010) found a net decrease in CDN in the N. Pacific ($-2\,\%$) in the $1\times$ geoscenario, which none of the models considered here recreate. The three models considered in this work also predict larger changes than found by Korhonen et al. (2010) in the other regions, with all regions experiencing a change of at least 55 % (cf. $\leq 20\,\%$ from Korhonen et al., 2010) with larger changes occurring when more particles are injected. The offline calculation of geoengineering used here is simpler than the wind speed dependent online calculation of Korhonen et al. (2010) but as the same net increase in aerosol number is used and the same updraught velocity is assumed the studies are broadly comparable. Differences in the simulated change in CDN could arise from differences in the simulated background aerosol distribution but GLOMAP-Mode and GLOMAP-Bin simulations are compared in detail in (Mann et al., 2012) which found that GLOMAP-Mode predicts between 25–100 % more CCN and thus would be expected to produce a smaller increase in CDN than GLOMAP-Bin. We therefore conclude that the main reason for the discrepancy is that Korhonen et al. (2010) used the activation parameterisation of Nenes and Seinfeld (2003) without the additional treatment of giant CCN of Barahona et al. (2010), which is used in this work (BN10). We propose that the suppression of supersaturation responsible for the small increase in CDN in Korhonen et al. (2010) was overestimated without this treatment.

4.1 Exploring the dependence on injection diameter and width

In the 0-D simulations a dependency on the efficiency of geoengineering on the diameter of the injected particles was apparent (Fig. 2), to explore this effect in the global models Fig. 6 shows the regional median geoengineered CDN concentration in the North Atlantic when a range of injection diameters (100–360 nm) is used. In this figure we fix the number of injected particles (at 300 particles cm^{-3}) and alter the diameter of injection. This has the effect of increasing the mass of aerosol emitted as the diameter is increased. The three other target regions show a similar dependency so are not shown.

None of the models show a strong dependence of CDN on the injection diameter, but all models show that an injection diameter of 100 nm is the least efficient as particles of this size are too small to activate when supersaturations are low. An injection diameter of 160 nm is found to be the most efficient in all models and in all regions. Increasing the injection diameter above 160 nm leads to a smaller increase in CDN,

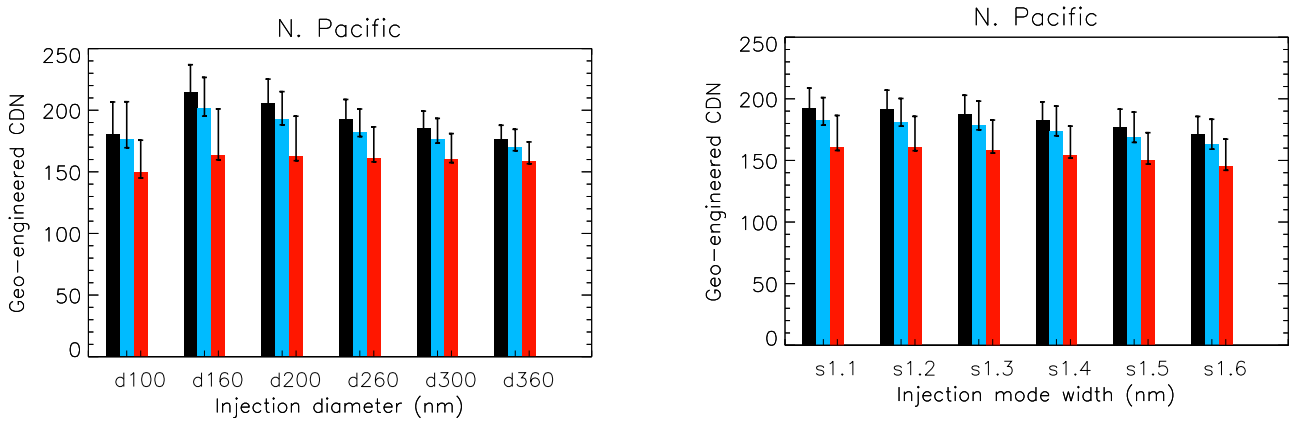

Fig. 6. The median geoengineered CDN concentration in the N. Pacific in GLOMAP (black), EMAC (blue) and ECHAM-HAM (red) arising from the injection of a narrow mode ($\sigma = 1.1$) of 300 particles cm^{-3}. In **(a)** the dry diameter of the injected mode is increased from 100–360 nm (x-axis) and in **(b)** the standard deviation of the injected mode is increased from 1.1 to 1.6. Error bars show the 25 and 75 percentiles.

despite the increase in the total mass of the injected particles. The importance of injection size is model dependent with GLOMAP and EMAC showing moderate sensitivity (reduction in CDN of 13 %, d360 compared to d160 nm) but ECHAM-HAM a lower sensitivity (3 %). The most efficient diameter for injection depends on the background aerosol distribution (Fig. 2) thus the weak dependence is largely due to averaging effects as in some locations an increase in injection diameter increases CDN and in others a decrease occurs, the net effect is therefore small. The sensitivity of the CDN to the choice of aerosol model is as large as the sensitivity to the injection size within each individual model (for d160 nm and above).

The dependence on injection diameter is different to that of Partanen et al. (2012) who investigated the sensitivity to injection diameter by holding the mass of aerosol injected constant, they found an injection diameter of 100 nm to be more efficient than an injection diameter of 260 nm. As Partanen et al. (2012) held the injected mass constant the calculated sensitivity to injection size is dominated by the fact that a reduction in particle size results in an increase in the number of particles injected. Here we find that for a constant number there is some additional sensitivity to injected size.

In the simulations so far we have considered the injection of a very narrow aerosol mode ($\sigma = 1.1$), injection of a narrow mode is technically challenging thus in Fig. 6 we also consider the injection of increasingly wide modes ($\sigma = 1.1$ to 1.6). The three models all predict a similar reduction in the geoengineered CDN concentration as the geometric standard deviation of the injected mode is increased, but the effect is small: the multi-model mean reduction in geoengineered CDN moving from $\sigma = 1.1$ to $\sigma = 1.6$ is 10 %, which is small compared to the difference between models.

4.2 Exploring the maximum possible increase in CDN

Although the 350 particles cm^{-3} (5 × geoscenario) is already a large perturbation to the pre-existing marine aerosol, it may be possible to increase the number of advertently introduced aerosol further. To explore this possibility Fig. 7 shows the absolute CDN concentration in the three models in a range of increasingly intensive geoengineering scenarios. We present results in the four target regions previously identified as being suitable for geoengineering due to their extensive cloud cover (Salter et al., 2008, marked on Fig. 5) and assuming four updraught velocities ($w = 0.05, 0.10, 0.20, 0.40$ m s^{-1}). In the presence of intensive geoengineering (increases of > 400 particles cm^{-3}) the absolute CDN simulated by the three models is very similar as the advertently introduced particle number dominates over background number concentrations. In all three models increasing the number of advertently introduced aerosol results in an increase in the CDN concentration with the overall shape of the aerosol number/CDN relationship similar to that found in previous measurement (Martin et al., 1994; Ramanathan et al., 2001) and model (Jones et al., 2001; Pringle et al., 2009) studies.

The extent of the increase in CDN is influenced by the in-cloud updraught velocity. At low updraughts (≤ 0.1 m s^{-1}) the CDN increases with the number of particles injected up to 400–600 cm^{-3}, above this injection number updraught as a source of saturation becomes the limiting factor and the scope for further increases in CDN becomes limited. With an in-cloud updraught velocity of 0.2 m s^{-1} this limited regime does not appear until ≥ 800 cm^{-3} are injected. A similar "updraught-limited" regime was identified by Reutter et al. (2009) who found that in pyro-convective conditions activation became updraught limited when the ratio of the updraught velocity to the aerosol number concentration was sufficiently small. Figure 7 shows that this updraught limited

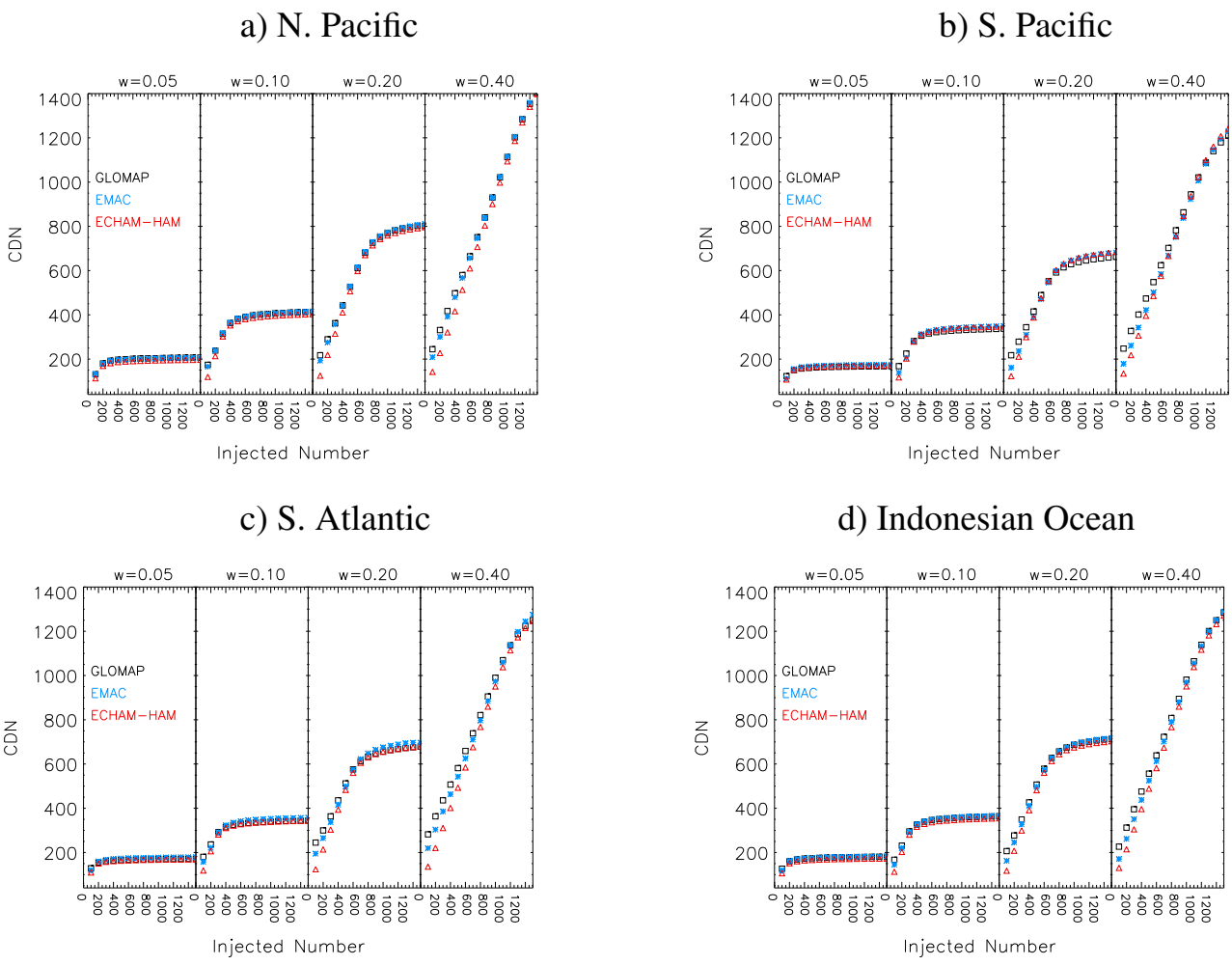

Fig. 7. Absolute CDN as a function of in-cloud updraught velocity (see top x-axis) and injected aerosol number (bottom x-axis). The geoengineered aerosol is assumed to have a modal diameter of 260 nm and a geometric standard deviation of 1.1 (black square), 1.3 (blue star) and 1.6 (red triangle).

regime also occurs in very intensive geoengineering scenarios and limits the maximum possible increase in CDN.

To avoid the uncertainty of calculating fields of background and geoengineered CDN, some previous studies have assumed that a geoengineered CDN concentration of 375 (or 1000 cm^{-3}) is uniformly possible (Latham et al., 2008; Jones et al., 2009; Rasch et al., 2009). They found that this CDN concentration was sufficient to offset either all, or a significant fraction of the radiative forcing in a double CO_2 scenario. Figure 8 shows histograms of the multi-model absolute CDN concentration in a range of geoengineering scenarios and assumed updraught velocities, the vertical dotted line marks the 375 cm^{-3} threshold and only gridboxes with a low level cloud cover of $> 50\,\%$ have been considered (cloud cover taken from the ISCCP low cloud data). As we do not consider the processes of collision coalescence this CDN at cloud base is an upper limit of the maximum feasible CDN concentration at cloud top. This limitation is particularly important at higher updrafts as it is with these updrafts that rain formation is more likely to occur, which would decrease CDN.

If the updraught velocity is $\geq 0.2\,\mathrm{m\,s}^{-1}$ an enhancement in aerosol number concentration of $\geq 400\,\mathrm{cm}^{-3}$ is sufficient to achieve a CDN concentration of 375 cm^{-3} in all gridboxes in all models, this is slightly larger than the online enhancement calculated in the 5 × geoscenario calculated by Korhonen et al. (2010, 365 cm^{-3}), but with this enhancement and updraught the CDN is substantially over 375 cm^{-3}, with a mean CDN concentration of 440 cm^{-3}. Updraught limitation becomes important at lower updraughts: when $w = 0.1\,\mathrm{m\,s}^{-1}$ an enhancement of 400 cm^{-3} results in a CDN of $> 375\,\mathrm{cm}^{-3}$ in only 49 % of gridboxes and when $w = 0.05\,\mathrm{m\,s}^{-1} < 1\,\%$ of gridboxes have a CDN of $> 375\,\mathrm{cm}^{-3}$.

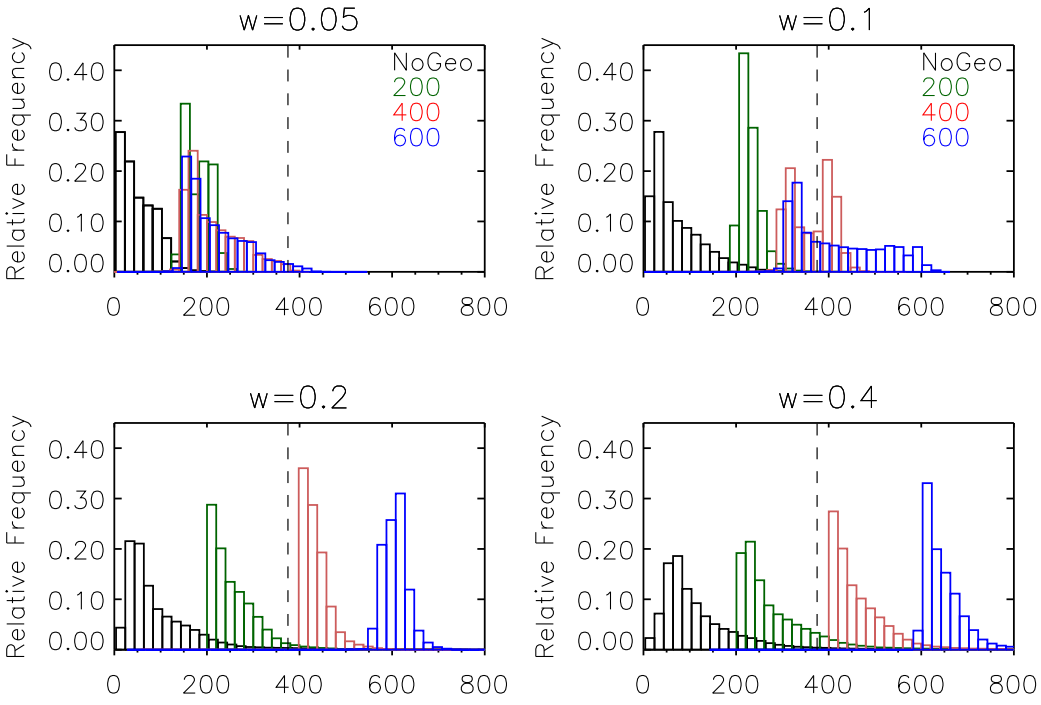

Fig. 8. Histograms showing the absolute CDN at cloud base predicted: black) in the absence of geoengineering and also with an injection of (green) 200 cm^{-3}, (red) 400 cm^{-3}, (blue) 700 cm^{-3}. Histograms are calculated using data from all the three aerosol models combined: GLOMAP, EMAC and ECHAM-HAM and show calculations assuming 4 different updraught velocities: (top left) $w = 0.05$, (top right) $w = 0.10$, (bottom left) $w = 0.20$, (bottom right) $w = 0.40\,m\,s^{-1}$.

At the updraughts considered a CDN of of 1000 cm^{-3} is almost never achieved.

As updraughts of $\leq 0.2\,m\,s^{-1}$ are common in marine stratocumulus clouds (e.g. Guibert et al., 2003; Lu et al., 2007; Guo et al., 2008) assuming a global mean value of 375 cm^{-3} is likely to overestimate the geoengineered CDN concentration and result in an overestimation of the potential cooling efficiency of sea-spray geoengineering, however the importance of this effect will depend on the spectrum of updraught velocities in the geoengineered clouds, which is better examined using a cloud resolving model, or through dedicated field campaigns. In conclusion, we see from Figs. 7 and 8 that the three models examined here show that there is scope for larger regional increases in CDN than achieved in Korhonen et al. (2010), but in all models when the updraught is assumed to be low there is a natural limitation to the increase in CDN attainable. Calculations of the percentage increase in CDN must therefore consider the frequency distribution of updraughts in marine stratocumulus clouds in greater detail.

5 Conclusions

Sea spray geoengineering of marine stratocumulus clouds to increase cloud albedo has been proposed as a possible technique to slow the rate of warming due to anthropogenic greenhouse gases. We have presented an investigation into the ability of geoengineered aerosol to activate to form cloud droplets and thus increase cloud droplet number. The efficacy has been explored in a 0-D box model scenario and also diagnosed from the aerosol fields simulated by three global aerosol models.

In the 0-D simulations we find that, in line with previous studies, the ability of the additional aerosol to activate depends on: (i) the properties of the additional aerosol, (ii) the background aerosol concentrations and (iii) the in-cloud updraught velocity. As would be expected, the increase in CDN is greatest when the background aerosol loading is low as there is little competition for water vapour. We do not find large regions of parameter space where decreases in CDN occur as a result of geoengineering, but it can happen when at least three of the following conditions are met: the injected particle number is $< 100\,cm^{-3}$, the injected diameter is > 250–300 nm, the background aerosol loading is large ($\geq 150\,cm^{-3}$) and the in-cloud updraught velocity is low ($< 0.2\,m\,s^{-1}$). The finding that the injection of a small number of particles can decrease CDN is interesting as, close

to a ship, the enhancement of aerosol concentrations is expected to be large but, further from the ship, dilution effects will become important and the increase in aerosol number is likely to be more modest, leading to aerosol number concentrations which may decrease CDN. High resolution modelling or field experiments would be required to assess the magnitude of this finding in more detail.

By examining output from three established global aerosol models we are able to examine the sensitivity of the predicted change in CDN to the aerosol model used. We find that the simulated percentage increase in CDN varies substantially between the three models with ECHAM-HAM predicting the largest percentage increase in CDN and GLOMAP-Mode the smallest. The inter-model differences are due to the range of background CDN concentrations simulated, which strongly affects the percentage change in CDN arising from geoengineering. In the absence of geoengineering, the global distribution of CDN is similar to the distribution of accumulation mode ($50 < R_p < 500$ nm) particles, which is similar in the models at the surface layer, but varies significantly at cloud base (here assumed to be 940 hPa) where fewer observations are available to constrain models. The inter-model differences in the predicted change in CDN can be as large as the regional differences, thus careful examination of the robustness of the background distribution is essential in studies that aim to predict the change in CDN that occurs as a result of geoengineering and where possible output from multiple models should be used.

The three models show quite weak dependence on the injected aerosol diameter and mode width. For a fixed injection number of 300 particles cm^{-3} injecting at a diameter of 160 nm diameter gives the largest increase in CDN, injecting at larger sizes decreases the enhancement in CDN (despite the increase in the mass of aerosol injected) but the effect is quite weak. Injecting a narrow mode of sea-spray aerosol ($\sigma = 1.1$) gives the largest increase in CDN, but when the modal geometric standard deviation is increased (to 1.6) only a small reduction in the predicted increase in CDN occurs.

We find that the in-cloud updraught velocity provides a natural limit to the maximum increase in CDN achievable through geoengineering. When the updraught is $\geq 0.2\,m\,s^{-1}$ injection of $400\,cm^{-3}$ particles results in a CDN concentration of $> 375\,cm^{-3}$ in all model gridboxes (with monthly mean cloud cover of $> 50\,\%$), but when the updraught is $0.1\,m\,s^{-1}$ the CDN is $> 375\,cm^{-3}$ in only 49 % of gridboxes. Updraught velocities of 0.1–0.2 $m\,s^{-1}$ are common in marine stratocumulus clouds thus it is likely that many clouds will fall between these two scenarios (i.e. 49–100 %) but this will depend on the properties of the perturbed cloud. Overall we conclude that the response to a large increase in aerosol number ($\geq 400\,cm^{-3}$) will depend critically on whether the updraught is at the higher or lower end of the range of updraughts possible in marine stratocumulus clouds and this should be considered in global studies.

This study only examines the response of the number of activated aerosol to the injected particles, in order to assess the climate impact one needs to also consider the change in albedo that arises from the geoengineering. This is dependent on the cloud liquid water response, the initial cloud albedo and the simulated cloud cover. Further work examining the model dependence of these properties is required for a robust assessment of the efficiency of sea spray geoengineering.

Acknowledgements. We thank the AeroCom aerosol model inter-comparison project for the provision of the global model data used in this study and the development team behind each model. We also thanks A. Nenes for provision of the activation parametrisation code, H. Korhonen for provision of model data and useful discussion and Adrian Lock for provision of the ASTEX simulation diagnostics. P. Stier has been supported by the Geoengineering Programme of the Oxford Martin School.

Edited by: J. H. Seinfeld

References

Akbari, H., Menon, S., and Rosenfeld, A.: Global cooling: increasing world-wide urban albedos to offset CO_2, Clim. Change, 94, 275–286, doi:10.1007/s10584-008-9515-9, 2009.

Alterskjær, K., Kristjánsson, J. E., and Seland, Ø.: Sensitivity to deliberate sea salt seeding of marine clouds – observations and model simulations, Atmos. Chem. Phys., 12, 2795–2807, doi:10.5194/acp-12-2795-2012, 2012.

Barahona, D., West, R. E. L., Stier, P., Romakkaniemi, S., Kokkola, H., and Nenes, A.: Comprehensively accounting for the effect of giant CCN in cloud activation parameterizations, Atmos. Chem. Phys., 10, 2467–2473, doi:10.5194/acp-10-2467-2010, 2010.

Bennartz, R.: Global assessment of marine boundary layer cloud droplet number concentration from satellite, J. Geophys. Res.-Atmos., 112, D02201, doi:10.1029/2006JD007547, 2007.

Bower, K., Choularton, T., Latham, J., Sahraei, J., and Salter, S.: Computational assessment of a proposed technique for global warming mitigation via albedo-enhancement of marine stratocumulus clouds, Atmos. Res., 82, 328–336, doi:10.1016/j.atmosres.2005.11.013, 2006.

Bretherton, C. S., Krueger, S. K., Wyant, M. C., Bechtold, P., Van Meijgaard, E., Stevens, B., and Teixeira, J.: A GCSS Boundary-Layer Cloud Model Intercomparison Study Of The First Astex Lagrangian Experiment, Boundary-Lay. Meteorol., 93, 341–380, doi:10.1023/A:1002005429969, 1999.

Bretherton, C. S., Wood, R., George, R. C., Leon, D., Allen, G., and Zheng, X.: Southeast Pacific stratocumulus clouds, precipitation and boundary layer structure sampled along 20S during VOCALS-REx, Atmos. Chem. Phys., 10, 10639–10654, doi:10.5194/acp-10-10639-2010, 2010.

Chen, Y. and Penner, J. E.: Uncertainty analysis for estimates of the first indirect aerosol effect, Atmos. Chem. Phys., 5, 2935–2948, doi:10.5194/acp-5-2935-2005, 2005.

Christensen, M. W. and Stephens, G. L.: Microphysical and macrophysical responses of marine stratocumulus polluted by

underlying ships: Evidence of cloud deepening, J. Geophys. Res.-Atmos., 116, D03201, doi:10.1029/2010JD014638, 2011.

Christensen, M. W., Coakley, J. A., and Tahnk, W. R.: Morning-to-Afternoon Evolution of Marine Stratus Polluted by Underlying Ships: Implications for the Relative Lifetimes of Polluted and Unpolluted Clouds, J. Atmos. Sci., 66, 2097, doi:10.1175/2009JAS2951.1, 2009.

Coakley, Jr., J. A. and Walsh, C. D.: Limits to the Aerosol Indirect Radiative Effect Derived from Observations of Ship Tracks., J. Atmos. Sci., 59, 668–680, doi:10.1175/1520-0469(2002)059¡0668:LTTAIR¿2.0.CO;2, 2002.

Crutzen, P. J.: Albedo Enhancement by Stratospheric Sulfur Injections: A Contribution to Resolve a Policy Dilemma?, Clim. Change, 77, 211–220, doi:10.1007/s10584-006-9101-y, 2006.

Fountoukis, C. and Nenes, A.: Continued development of a cloud droplet formation parameterization for global climate models, J. Geophys. Res.-Atmos., 110, D11212, doi:10.1029/2004JD005591, 2005.

Ghan, S. J., Guzman, G., and Abdul-Razzak, H.: Competition between Sea Salt and Sulfate Particles as Cloud Condensation, J. Atmos. Sci., 55, 3340–3347, 1998.

Guibert, S., Snider, J. R., and Brenguier, J.-L.: Aerosol activation in marine stratocumulus clouds: 1. Measurement validation for a closure study, J. Geophys. Res.-Atmos., 108, 8628, doi:10.1029/2002JD002678, 2003.

Guo, H., Liu, Y., Daum, P. H., Senum, G. I., and Tao, W.: Characteristics of vertical velocity in marine stratocumulus: comparison of large eddy simulations with observations, Environ. Res. Lett., 3, 045020, doi:10.1088/1748-9326/3/4/045020, 2008.

Hawkins, L. N., Russell, L. M., Twohy, C. H., and Anderson, J. R.: Uniform particle-droplet partitioning of 18 organic and elemental components measured in and below DYCOMS-II stratocumulus clouds, J. Geophys. Res.-Atmos., 113, 14201, doi:10.1029/2007JD009150, 2008.

Heintzenberg, J. and Larssen, S.: Structure, variability and persistence of the submicrometer marine aerosol, Tellus, 56, 357–367, 2004.

Hill, A. A., Feingold, G., and Jiang, H.: The Influence of Entrainment and Mixing Assumption on Aerosol-Cloud Interactions in Marine Stratocumulus, J. Atmos. Sci., 66, 1450, doi:10.1175/2008JAS2909.1, 2009.

Hobbs, P. V., Garrett, T. J., Ferek, R. J., Strader, S. R., Hegg, D. A., Frick, G. M., Hoppel, W. A., Gasparovic, R. F., Russell, L. M., Johnson, D. W., O'Dowd, C., Durkee, P. A., Nielsen, K. E., and Innis, G.: Emissions from Ships with respect to Their Effects on Clouds., J. Atmos. Sci., 2570–2590, doi:10.1175/1520-0469(2000)057¡2570:EFSWRT¿2.0.CO;2, 2000.

Jöckel, P., Tost, H., Pozzer, A., Brühl, C., Buchholz, J., Ganzeveld, L., Hoor, P., Kerkweg, A., Lawrence, M. G., Sander, R., Steil, B., Stiller, G., Tanarhte, M., Taraborrelli, D., van Aardenne, J., and Lelieveld, J.: The atmospheric chemistry general circulation model ECHAM5/MESSy1: consistent simulation of ozone from the surface to the mesosphere, Atmos. Chem. Phys., 6, 5067–5104, doi:10.5194/acp-6-5067-2006, 2006.

Jones, A., Roberts, D., Woodage, M., and Johnson, C.: Indirect sulphate aerosol forcing in a climate model with an interactive sulphur cycle, J. Geophys. Res.-Atmos., 106, 20293–20310, 2001.

Jones, A., Haywood, J., and Boucher, O.: Climate impacts of geoengineering marine stratocumulus clouds, J. Geophys. Res.-Atmos., 114, 10106, doi:10.1029/2008JD011450, 2009.

Karydis, V. A., Kumar, P., Barahona, D., Sokolik, I. N., and Nenes, A.: On the effect of dust particles on global cloud condensation nuclei and cloud droplet number, J. Geophys. Res., 116, D23204, doi:10.1029/2011JD016283, 2011.

Korhonen, H., Carslaw, K. S., and Romakkaniemi, S.: Enhancement of marine cloud albedo via controlled sea spray injections: a global model study of the influence of emission rates, microphysics and transport, Atmos. Chem. Phys., 10, 4133–4143, doi:10.5194/acp-10-4133-2010, 2010.

Latham, J. and Smith, M. H.: Effect on global warming of wind-dependent aerosol generation at the ocean surface, Nature, 13, 372–373, 1990.

Latham, J., Rasch, P., Chen, C., Kettles, L., Gadian, A., Gettelman, A., Morrison, H., Bower, K., and Choularton, T.: Global temperature stabilization via controlled albedo enhancement of low-level maritime clouds, Royal Society of London Philosophical Transactions Series A, 366, 3969–3987, doi:10.1098/rsta.2008.0137, 2008.

Lu, M. and Seinfeld, J. H.: Study of the Aerosol Indirect Effect by Large-Eddy Simulation of Marine Stratocumulus., J. Atmos. Sci., 62, 3909–3932, doi:10.1175/JAS3584.1, 2005.

Lu, M. and Seinfeld, J. H.: Effect of aerosol number concentration on cloud droplet dispersion: A large-eddy simulation study and implications for aerosol indirect forcing, J. Geophys. Res.-Atmos., 111, D02207, doi:10.1029/2005JD006419, 2006.

Lu, M., Conant, W. C., Jonsson, H. H., Varutbangkul, V., Flagan, R. C., and Seinfeld, J. H.: The Marine Stratus/Stratocumulus Experiment (MASE): Aerosol-cloud relationships in marine stratocumulus, J. Geophys. Res.-Atmos., 112, D10209, doi:10.1029/2006JD007985, 2007.

Mann, G. W., Carslaw, K. S., Spracklen, D. V., Ridley, D. A., Manktelow, P. T., Chipperfield, M. P., Pickering, S. J., and Johnson, C. E.: Description and evaluation of GLOMAP-mode: a modal global aerosol microphysics model for the UKCA composition-climate model, Geoscientific Model Development, 3, 519–551, doi:10.5194/gmd-3-519-2010, 2010.

Mann, G. W., Carslaw, K. S., Ridley, D. A., Spracklen, D. V., Pringle, K. J., Merikanto, J., Korhonen, H., Schwarz, J. P., Lee, L. A., Manktelow, P. T., Woodhouse, M. T., Schmidt, A., Breider, T. J., Emmerson, K. M., Reddington, C. L., Chipperfield, M. P., and Pickering, S. J.: Intercomparison of modal and sectional aerosol microphysics representations within the same 3-D global chemical transport model, Atmos. Chem. Phys., 12, 4449–4476, doi:10.5194/acp-12-4449-2012, 2012.

Martin, G., Johnson, D., and Spice, A.: The measurement and parameterization of effective radius of droplets in warm stratiform clouds, J. Atmos. Sci., 51, 1823–1842, 1994.

Merikanto, J., Spracklen, D. V., Pringle, K. J., and Carslaw, K. S.: Effects of boundary layer particle formation on cloud droplet number and changes in cloud albedo from 1850 to 2000, Atmos. Chem. Phys., 10, 695–705, doi:10.5194/acp-10-695-2010, 2010.

Meskhidze, N., Nenes, A., Conant, W. C., and Seinfeld, J.: Evaluation of a new Cloud Droplet Activation Parameterization with In Situ Data from CRYSTAL-FACE and CSTRIPE, J. Geophys. Res.-Atmos., 110, D16202, doi:10.1029/2004JD005703, 2005.

Morales, R. and Nenes, A.: Characteristic updrafts for computing distribution-averaged cloud droplet number and stratocumulus cloud properties, J. Geophys. Res.-Atmos., 115, D18220,

doi:10.1029/2009JD013233, 2010.

Nenes, A. and Seinfeld, J. H.: Parameterization of cloud droplet formation in global climate models, J. Geophys. Res.-Atmos., 108, D14, doi:10.1029/2002JD002911, 2003.

Parkes, B., Gadian, A., and Latham, J.: The Effects of Marine Cloud Brightening on Seasonal Polar Temperatures and the Meridional Heat Flux, ISRN Geophys., 2012, 142872, doi:10.5402/2012/142872, 2012.

Partanen, A.-I., Kokkola, H., Romakkaniemi, S., Kerminen, V.-M., Lehtinen, K. E. J., Bergman, T., Arola, A., and Korhonen, H.: Direct and indirect effects of sea spray geoengineering and the role of injected particle size, J. Geophys. Res., 117, D02203, doi:10.1029/2011JD016428, 2012.

Peng, Y., Lohmann, U., and Leaitch, R.: Importance of vertical velocity variations in cloud droplet nucleation process of marine stratus clouds, J. Geophys. Res.-Atmos., 110, doi:10.1029/2004JD004922, 2005.

Pozzer, A., de Meij, A., Pringle, K. J., Tost, H., Doering, U. M., van Aardenne, J., and Lelieveld, J.: Distributions and regional budgets of aerosols and their precursors simulated with the EMAC chemistry-climate model, Atmos. Chem. Phys., 12, 961–987, doi:10.5194/acp-12-961-2012, 2012.

Pringle, K. J., Carslaw, K. S., Spracklen, D. V., Mann, G. M., and Chipperfield, M. P.: The relationship between aerosol and cloud drop number concentrations in a global aerosol microphysics model, Atmos. Chem. Phys., 9, 4131–4144, doi:10.5194/acp-9-4131-2009, 2009.

Pringle, K. J., Tost, H., Message, S., Steil, B., Giannadaki, D., Nenes, A., Fountoukis, C., Stier, P., Vignati, E., and Lelieveld, J.: Description and evaluation of GMXe: a new aerosol submodel for global simulations (v1), Geosci. Model Dev., 3, 391–412, doi:10.5194/gmd-3-391-2010, 2010.

Rahn, D. A. and Garreaud, R.: Marine boundary layer over the subtropical southeast Pacific during VOCALS-REx. Part 1: Mean structure and diurnal cycle, Atmos. Chem. Phys., 10, 4491–4506, doi:10.5194/acp-10-4491-2010, 2010.

Ramanathan, V., Crutzen, P., Kiehl, J., and Rosenfeld, D.: Atmosphere – Aerosols, climate, and the hydrological cycle, Science, 294, 2119–2124, 2001.

Rasch, P. J., Latham, J., and Chen, C.-C. J.: Geoengineering by cloud seeding: influence on sea ice and climate system, Environ. Res. Lett., 4, 045112, http://stacks.iop.org/1748-9326/4/i=4/a=045112, 2009.

Reutter, P., Su, H., Trentmann, J., Simmel, M., Rose, D., Gunthe, S. S., Wernli, H., Andreae, M. O., and Pöschl, U.: Aerosol- and updraft-limited regimes of cloud droplet formation: influence of particle number, size and hygroscopicity on the activation of cloud condensation nuclei (CCN), Atmos. Chem. Phys., 9, 7067–7080, doi:10.5194/acp-9-7067-2009, 2009.

Salter, S., Sortino, G., and Latham, J.: Sea-going hardware for the cloud albedo method of reversing global warming, Royal Society of London Philosophical Transactions Series A, 366, 3989–4006, doi:10.1098/rsta.2008.0136, 2008.

Segrin, M. S., Coakley, J. A., and Tahnk, W. R.: MODIS Observations of Ship Tracks in Summertime Stratus off the West Coast of the United States, J. Atmos. Sci., 64, 4330, doi:10.1175/2007JAS2308.1, 2007.

Spracklen, D., Pringle, K., Carslaw, K., Chipperfield, M., and Mann, G.: A global off-line model of size resolved aerosol processes; I. Model development and prediction of aerosol properties, Atmos. Chem. Phys., 5, 2227–2252, doi:10.5194/acp-5-2227-2005, 2005.

Stier, P., Feichter, J., Kinne, S., Kloster, S., Vignati, E., Wilson, J., Ganzeveld, L., Tegen, I., Wener, M., Balkanski, Y., Schulz, M., and Boucher, O.: The aerosol-climate model ECHAM5-HAM, Atmos. Chem. Phys., 5, 1125–1156, doi:10.5194/acp-5-1125-2005, 2005.

Textor, C., Schulz, M., Guibert, S., Kinne, S., Balkanski, Y., Bauer, S., Berntsen, T., Berglen, T., Boucher, O., Chin, M., Dentener, F., Diehl, T., Easter, R., Feichter, H., Fillmore, D., Ghan, S., Ginoux, P., Gong, S., Grini, A., Hendricks, J., Horowitz, L., Huang, P., Isaksen, I., Iversen, I., Kloster, S., Koch, D., Kirkevåg, A., Kristjansson, J. E., Krol, M., Lauer, A., Lamarque, J. F., Liu, X., Montanaro, V., Myhre, G., Penner, J., Pitari, G., Reddy, S., Seland, Ø., Stier, P., Takemura, T., and Tie, X.: Analysis and quantification of the diversities of aerosol life cycles within AeroCom, Atmos. Chem. Phys., 6, 1777–1813, doi:10.5194/acp-6-1777-2006, 2006.

Twomey, S.: The Influence of Pollution on the Shortwave Albedo of Clouds., J. Atmos. Sci., 34, 1149–1154, doi:10.1175/1520-0469(1977)034¡1149:TIOPOT¿2.0.CO;2, 1977.

Twomey, S.: Aerosols, clouds and radiation, Atmos. Environ., part A: General Topics, 25, 2435–2442, doi:10.1016/0960-1686(91)90159-5, 1991.

Vignati, E., Wilson, J., and Stier, P.: M7: An efficient size-resolved aerosol microphysics module for large-scale aerosol transport models, J. Geophys. Res., 109, D22, doi:10.1029/2003JD004485, 2004.

Wang, H., Rasch, P. J., and Feingold, G.: Manipulating marine stratocumulus cloud amount and albedo: a process-modelling study of aerosol-cloud-precipitation interactions in response to injection of cloud condensation nuclei, Atmos. Chem. Phys., 11, 4237–4249, doi:10.5194/acp-11-4237-2011, 2011.

Zhang, K., O'Donnell, D., Kazil, J., Stier, P., Kinne, S., Lohmann, U., Ferrachat, S., Croft, B., Quaas, J., Wan, H., Rast, S., and Feichter, J.: The global aerosol-climate model ECHAM-HAM, version 2: sensitivity to improvements in process representations, Atmos. Chem. Phys., 12, 8911–8949, doi:10.5194/acp-12-8911-2012, 2012.